J Electr Eng Technol.2017; 12(5): 1777-1788
http://doi.org/10.5370/JEET.2017.12.5.1777

ISSN(Print) 1975-0102
ISSN(Online) 2093-7423

Design and Dynamic Performance Analysis of a Stand-alone Microgrid – A Case Study of Gasa Island, South Korea

Munir Husein*, Vu Ba Hau*, Il-Yop Chung†, Woo-Kyu Chae and Hak-Ju Lee****

Abstract – This paper presents the design and dynamic analysis of a stand-alone microgrid with high penetration of renewable energy. The optimal sizing of various components in the microgrid is obtained considering two objectives: minimization of levelized cost of energy (LCOE) and maximization of renewable energy penetration. Integrating high renewable energy in stand-alone microgrid requires special considerations to assure stable dynamic performance, we therefore develop voltage and frequency control method by coordinating Battery Energy Storage System (BESS) and diesel generators. This approach was applied to the design and development of Gasa Island microgrid in South Korea. The microgrid consists of photovoltaic panels, wind turbines, lithium-ion batteries and diesel generators. The dynamic performance of the microgrid during different load and weather variations is verified by simulation studies. Results from the real microgrid were then presented and discussed. Our approach to the design and control of microgrid will offer some lessons in future microgrid design.

Keywords: Microgrid, Economic analysis, Dynamic performance, Voltage control, Frequency control

1. Introduction

In most islands, due to the constraints imposed by features of terrain and costs associated with cabling of an electric supply network, it is unlikely that these places will ever enjoy benefits of interconnections to the main electric grid [1]. Electricity has been therefore provided primarily by diesel generators. However, because of the volatility in fuel prices and pollutant emission, many islands around the world are shifting to more environmentally friendly and sustainable energy solutions.

In recent years, there is an increase in the adoption of microgrids in islands [2]. The optimal design of microgrid has been reported using various performance models and optimization techniques [3]. In addition, various design software tools, like HOMER and iHoga, were developed. HOMER remains the most popular and is being widely used worldwide by both researchers and developers [4-5].

Most of the designs in the literature, including [6-13], do not consider dynamic performance as part of the design. This is an important consideration because stand-alone microgrids lack the voltage and frequency reference provided by the central grid. The dynamic performance becomes even more imperative in a stand-alone microgrid with high penetration of renewable energy. In these types of systems, voltage and frequency control method need to be developed in order to come up with a final design.

The conventional approach to voltage and frequency control in a stand-alone microgrid is to use diesel generators to set the nominal system frequency and voltage [14]. Stability is achieved by using active power/frequency (p/f) and reactive power/voltage (q/v) droop control. This approach is adopted from the conventional power system and has some weakness in small stand-alone microgrids because they have low system inertia.

Over the years, various methods of voltage and frequency control that does not depend on diesel generators were proposed. In [15-17], renewable energy sources (RESs) were used to control the system frequency. While this approach is attractive, economics dictates that energy from renewable sources should be fully utilized whenever available.

Recently, there is a growing interest in the use of Battery Energy Storage System (BESS) for frequency and voltage control in islanded microgrid. This interest is in part due to the continuous decline in the price of BESS. Studies were conducted to demonstrate the effectiveness of this method [18-22], however, all the works we have surveyed in the literature are verified by simulation or laboratory prototype. In addition, no economic analysis was performed in other to justify the adoption of this approach.

There are two challenges that must be addressed when using BESS for frequency control in standalone microgrid. First, its capacity should be large enough to work as the main source and an energy storage. Second, we need to confine its size due to its expensive installation and

† Corresponding Author: School of Electrical Engineering, Kookmin University, Seoul, Korea. (chung@kookmin.ac.kr)
* School of Electrical Engineering, Kookmin University, Seoul, Korea.
** Korea Electric Power Research Institute (KEPRI), 105 Munji-ro, Yuseong-gu, Daejeon 34056, Korea
Received: March 2, 2017; Accepted: May 29, 2017

Fig. 1. Photo of Gasa Island microgrid

maintenance costs. To deal with these ironical situations, we perform economic analysis for optimal size of BESS, diesel generators, and RESs.

In this paper, we approach microgrid design in two phase: sizing/economic analysis and dynamic analysis. In the sizing/economic analysis phase, we simulate various cases using HOMER software, and then use multiple objectives to select the optimal design. In the dynamic analysis, we developed voltage and frequency control method by coordinating BESS and diesel generators and simulate the system dynamic response in MATLAB/ Simulink environments.

Our approach to the design of microgrid is applied to Gasa Island microgrid constructed by Korea Electric Power Corporation (KEPCO). It is managed by automated energy management system (EMS), which tracks electricity use in real time, forecasts demand and channels power either to meet immediate demands or to store the surplus in the BESS.

The rest of the paper is organized as follows: section two provides a brief overview of Gasa Island: its description, energy demand and available RESs. In section three, various case studies are simulated in other to find an optimal configuration that satisfies design objectives. To guarantee stability and investigate dynamic performance, voltage and frequency control method methods are developed in section four. Simulation and operation results are discussed in section five, and, finally, a conclusion is drawn in section six.

2. Description and Energy Status of Gasa Island

Gasa Island is located approximately 6 km southwest of the Korean Peninsula. It currently has a population of 286 inhabitants in 168 households. Before the construction of the microgrid, the island is served by two 100 kW diesel generators operated in parallel during normal hours, and one additional standby generator. As of 2013, the average annual fuel consumption of the island is 285,000 L/year.

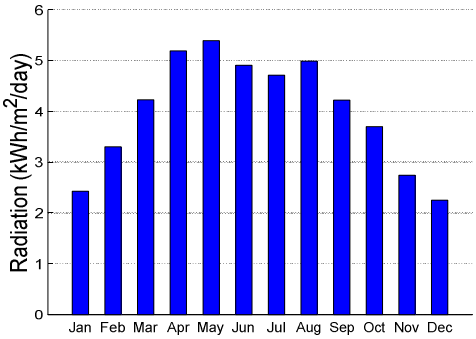

Fig. 2. Monthly average GHI at Gasa Island

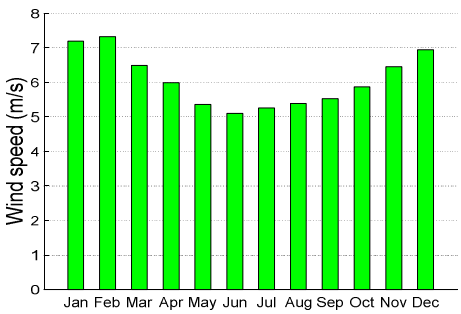

Fig. 3. Monthly average wind speed at Gasa Island

2.1 Analysis of renewable energy resources

According to solar radiation data downloaded from the NASA Surface Meteorology and Solar Energy website, the annual average solar radiation for this location is 4.01 kW/m²/day. Fig. 2 shows the monthly average global horizontal irradiance (GHI) over a one-year period. Annual average wind speed of Gasa Island is 6.07 m/s at 50 m above the sea level according to the database of NASA. Fig. 3 shows the wind speed profile over a period of one-year.

2.2 Analysis of demand

When designing stand-alone microgrid, it is of fundamental importance to analyze the loads that will be

Fig. 4. Average daily load profile of Gasa Island

connected to the microgrid and to estimate their temporal evolution. In Gasa Island, there are a school, a town hall, a lighthouse, and seaweed and fish farms in the island and the average loads is around 95 kW. The average load demand is 2,164 kWh/day and load factor is 0.48. Fig. 4 illustrates averaged monthly load of Gasa Island used for optimal design study.

3. Sizing and Economic Analysis Using HOMER

3.1 HOMER software and input data

HOMER (Hybrid Optimization of Multiple Energy Resources) is a microgrid analysis software originally developed at the U.S. National Renewable Energy Laboratory to simplify the task of designing microgrids. HOMER is now licensed to HOMER Energy. It models a power system's physical behavior and its life-cycle cost, which is the total cost of installing and operating the system over its lifespan. It then allows users to compare many different design options based on their technical and economic merits [23]. HOMER performs three principal tasks: simulation, optimization, and sensitivity analysis.

Tables 1 through 5 provide financial and component parameters needed to perform simulation and optimization in HOMER. Various configurations are simulated for a total project lifetime of 25 years. The results and discussion of this analysis are presented in the next section.

3.2 Results of sizing and economic analysis

We search for an optimal configuration of distributed energy resources that meet our design goal at the minimum cost. The design goal is the minimization of LCOE and maximization of renewable energy penetration (REP). LCOE is the average cost per kilowatt-hour of useful electrical energy produced by the system defined in [24] as:

$$LCOE = \frac{C_{tot}}{E_s + E_{grid}} \tag{1}$$

where C_{tot} is the total annualized cost, E_s is a total

Table 1. Project financial parameters.

Parameter	Value	Unit
Nominal interest rate	4.50	%
Real discount rate	3.26	%
Inflation rate	1.20	%
Project lifetime	25.0	years

Table 2. Photovoltaic parameters

Parameter	Value	Unit
Capital cost	3,000	$/kW
Replacement cost	2,500	$/kW
O&M cost	10.00	$/kW/year
Lifetime	25.0	years

Table 3. Wind turbine parameters

Parameter	Value	Unit
Capital cost	500,000	$/100kW
Replacement cost	400,000	$/100kW
O&M cost	5,000	$/100kW/year
Lifetime	20.0	years

Table 4. BESS and PCS parameters

Parameter	Value	Unit
Capital cost	700	$/kW
Replacement cost	500	$/kW
O&M cost	10	$/kW/year
Lifetime	10	years
PCS capital cost	300	$/kW
PCS replacement cost	300	$/kW
PCS O&M cost	0	$/kW/year
PCS lifetime	15	years

Table 5. Diesel generator parameters

Parameter	Value	Unit
Capital cost	500	$/kW
Replacement cost	500	$/kW
O&M cost	0.05	$/kW/hour
Lifetime	30,000	hours

electrical energy that the microgrid served, and E_{grid} is the total electricity sold to the grid. REP is the fraction of the energy delivered to the load that originated from renewable power sources, it is defined in [24] as:

$$REP = 1 - \frac{E_{nonren}}{E_s} \tag{2}$$

where E_{nonren} is the non-renewable electrical production, and E_s is as defined before. Another parameter of importance to this study is battery autonomy (BA), which is defined as the time for which battery can support the load when all other energy sources are unavailable. It is a function of battery SoC, capacity, and load size. We derive the value of battery autonomy as:

$$BA = \frac{Q_b \times \eta_b \times DOD}{E_L} \tag{3}$$

Table 6. Optimal sizing results

Case	BESS (kWh)	BESS PCS (kW)	Photovoltaic (kW)	Wind turbine (kW)	Diesel generator (kW)
Case 1	0	0	0	0	200
Case 2	0	0	400	0	200
Case 3	500	500	200	200	200
Case 4	2,000	500	400	100	200
Case 5	3,000	500	300	400	200
Case 6	5,000	500	400	400	0

Table 7. Performance simulation results

Case	LCOE ($/kWh)	REP (%)	Fuel consumption (L)	Fuel consumption reduction (%)	Battery autonomy (hours)
Case 1	0.558	0	227,604	0	0
Case 2	0.519	20	172,353	24.28	0
Case 3	0.422	63	81,140	64.35	3.96
Case 4	0.481	80	43,962	80.64	15.83
Case 5	0.556	94	12,709	94.42	23.75
Case 6	0.730	100	0	100	39.58

Table 8. Pollutant emissions results (all in kg.)

Case	Carbon dioxide	Carbon monoxide	Unburned hydrocarbons	Particulate matter	Sulfur dioxide	Nitrogen oxides
Case 1	599,356.10	1,479.43	163.87	111.53	1,203.61	13,201.03
Case 2	453,826.70	1,120.30	124.09	84.45	911.44	9,996.49
Case 3	213,667.54	527.41	58.42	39.76	429.08	4,706.10
Case 4	115,765.81	285.75	31.65	21.54	232.48	2,549.78
Case 5	33,673.62	83.12	9.21	6.27	67.62	741.67
Case 6	0	0	0	0	0	0

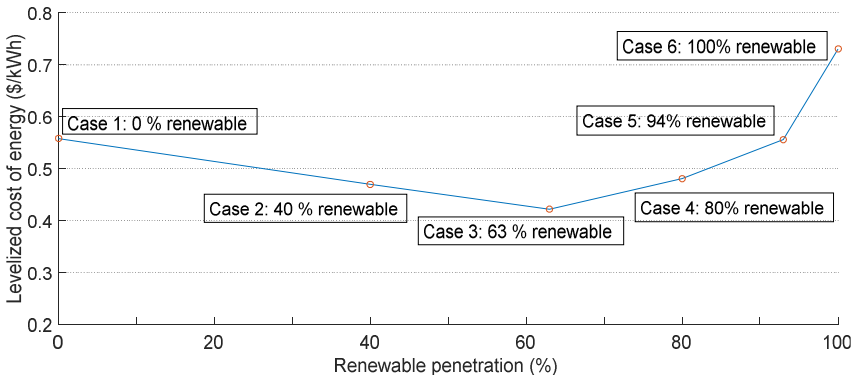

Fig. 5. LCOE vs. renewable energy penetration

where BA is battery autonomy in hours, Q_b is the nominal capacity of the battery bank (3 MWh), DOD is the depth of discharge (80 %), E_L is the average electrical load (96 kW in Gasa Island), and η_b is battery discharge efficiency (set to 95 %).

We modeled six different cases in HOMER and the results are presented in Table 6-8. Table 6 shows the optimal sizes of distributed energy resources (DER) of each case. The base case has only diesel generators, while other cases, with the exception of Case 6, has a combination of diesel generators and renewable energy components. Table 7 presents performance simulation results. The LCOE of the base case (diesel-only system) is 0.558 $/kWh. As REP increases, LCOE decreases due to the displacement of diesel fuel by renewable energy, as shown in Case 2. In Case 3, the lowest LCOE is reached at 63 % REP. Higher REP requires more storage and the cost of this storage increases the LCOE modestly as shown in Fig. 5. This reduces the economic attractiveness of the microgrid while substantially reducing the fuel consumption, which in turn will reduce emission. Beyond Case 5, at REP of around 94 %, LCOE surges sharply up to 0.73 in Case 6. This sudden rise is due to the bulk storage required to achieve 100 % REP. As renewable penetration is increasing, battery autonomy is also increasing, while fuel consumption is decreasing, thereby subsequently reducing pollutant emissions, as shown in Table 8.

3.3 Selection of optimal configuration

Case 1 is the base case, and LCOE of case 7 is unacceptably high and hence economically infeasible. The optimal case will, therefore, be chosen among case 2, 3, 4 and 5. The configuration with the lowest LCOE and highest REP will be selected as optimal. However, these are usually conflicting objectives, as can be seen in the results of this study: Case 3 has the lowest LCOE of 0.422 while Case 5 has the highest REP of 94 %. To choose between these cases, other benefits are considered, such as fuel consumption reduction, environmental effects, and battery autonomy.

Case 5 is selected as optimal for the following reasons: Fuel consumption reduction of case 5 is 94.42 %, compared to other cases, it is 24.28 % for case 2, 64.35 % for case 3, and 80.64 % for case 4. Emission reduction is one of the main reasons for adopting microgrids in islands. Table 8 shows the results of pollutant emissions of all cases. We find out case 5 reduces the pollutant emissions by 94 %, which is greater than that of all other cases. As we have pointed out in the introduction, BESS will be used as the main source to control system frequency. Therefore, its capacity should be large enough to work both as the main source and as an energy storage. Case 5 has has 3 MWh battery capacity, with autonomy of 23.75 hours, which is higher compared to other cases, as shown in Table 7.

4. Dynamic Performance Analysis

4.1 Architecture of the gasa island microgrid

Gasa Island microgrid employs modular distributed AC bus architecture on radial distribution lines. In this type of architecture, energy is supplied to the load from different points of the microgrid. These structures, even though provides flexibility in siting and expansion, causes the control to be more complicated than that of centralized architecture. Fig. 6 shows the location of the RESs in Gasa Island microgrid. The design goal of this microgrid is to replace diesel generators with RESs. Therefore, the power demand of the island can be fully supplied by eco-friendly RESs, and KEPCO can save the cost related to fuel consumption of diesel generators. The diesel generators operate only to maintain BESS SoC. Because the capacity of the BESS and its power conditioning system (PCS) is larger than diesel generators, it can be used as a master controller responsible for controlling voltage and frequency of the microgrid. Since the capacity of BESS is large enough, it can compensate the uncertainty and variation of the output of the RESs for a long time without diesel generators [24-25].

4.2 Voltage and frequency control methods

In conventional power systems, the frequency is directly

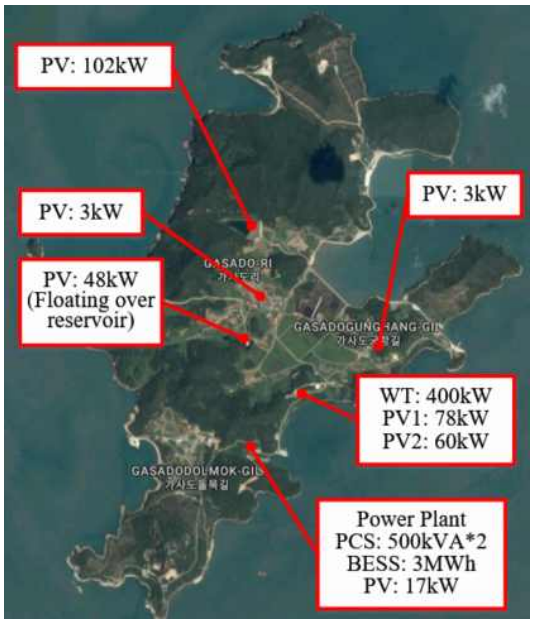

Fig. 6. Locations of distributed energy resources at Gasa Island

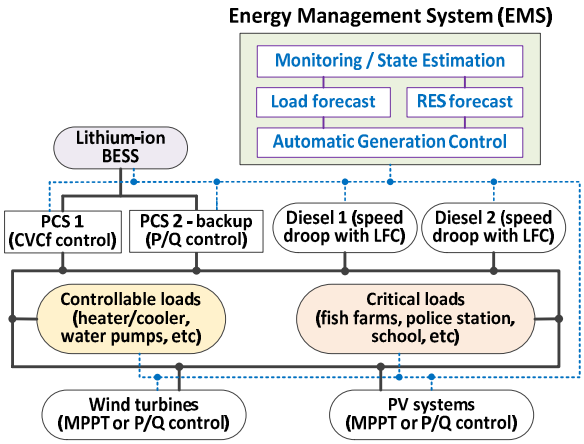

Fig. 7. Control concept of Gasa Island microgrid

related to the rotational speed of generator rotor, as can be seen from the swing equation [26]. If the system inertia is low, which is typical for small stand-alone microgrid, the system frequency is vulnerable to load change.

To avoid this problem, we used BESS to control system voltage and frequency instead of diesel generators. Fig. 7 illustrates the proposed control concept. One of two PCSs operates as the master controller that is responsible to constantly control the system voltage and frequency, therefore it is operated as a constant voltage and constant frequency (CVCF) mode. Another PCS is installed as a backup device of the master PCS and it can also operate in real and reactive power control (P/Q) mode during an emergency like SoC control of the BESS.

As discussed in the previous section, diesel generators turn on when the SoC of BESS is too low due to excessive discharge or during an emergency. The diesel generators

use speed droop control with load frequency control (LFC). The LFC signal of the diesel generators is manipulated by the system-wide EMS. The EMS predicts the output of RESs and load demands and determines on/off of the diesel generators and their exact amount of power generation. Therefore, the EMS conducts the functions of unit commitment and economic dispatch. The goal of optimization of the EMS is to maintain the daily average of the BESS SoC at 50%. For better performance, the EMS need to be able to limit the output of RESs and control the load demands.

4.3 Development of microgrid dynamic model

Gasa Island microgrid consists of wind turbines, photovoltaic arrays, battery energy storage system, diesel generators, and power electronics converters as illustrated in Fig. 8. The microgrid and power system network is modeled in MATLAB/Simulink. The nominal system frequency and voltage are 60 Hz and 380 V (line-to-line) at the generation bus and 6.9 kV at the distribution lines, respectively. The distribution line is a type ACSR 160-mm², 6.9-kV overhead cable. They are modeled as an equivalent circuit with inductance and resistance per-unit-length. The load is modeled as a combination of constant power load and dynamic load with a power factor of 0.9. The power electronics converters are modeled as two-level type average model. The inverter controllers provide the reference of three-phase sinusoidal voltages at the inverter terminal. We describe the modeling of all DER in the rest of this section.

4.3.1 BESS and PCS models

The lithium-ion battery dynamic model in reference [27] was used in this study. As discussed earlier, the BESS in Gasa Island has two operation modes: CVCF and P/Q control modes. The control circuit of the BESS PCS consists of phase locked loop (PLL), voltage controller, current controller, and pulse width modulation (PWM) reference signal generator [28]. The detailed functional block diagrams of BESS PCS controllers for the CVCF and P/Q mode are elaborated as the grid-forming and grid-feeding controllers, respectively in [18].

4.3.2 Diesel generator model

We model a diesel generator consisting of a synchronous machine, a turbine, a speed governor, and an exciter with an automatic voltage regulator (AVR) [29]. The turbine and the speed governor are models by a first-order transfer function. The governor controls the real power of the generator and system frequency with active power vs. frequency (P-f) droop characteristics. With this droop control concept, diesel generators can securely share the load variations with other generators with droop control. The AVR controls the reactive power and the terminal voltage of the generator by manipulating the field current. We used AC1A type AVR model and excitation model defined by IEEE Standard 421.1-2007 [30].

4.3.3 Photovoltaic system model

In this paper, one-diode equivalent circuit model is used for the photovoltaic module, which uses a current source in parallel with a diode. This model offers a compromise between simplicity and accuracy [31]. It is modeled by the following equation

$$I = I_{ph} - I_0\left[\exp\left(\frac{q(V - IR_s)}{kT_{cell}A}\right)\right] - \frac{V + IR_s}{R_{sh}} \quad (4)$$

where I is the PV output current (A), I_{ph} is photocurrent (A), I_0 is the reverse saturation current (A),

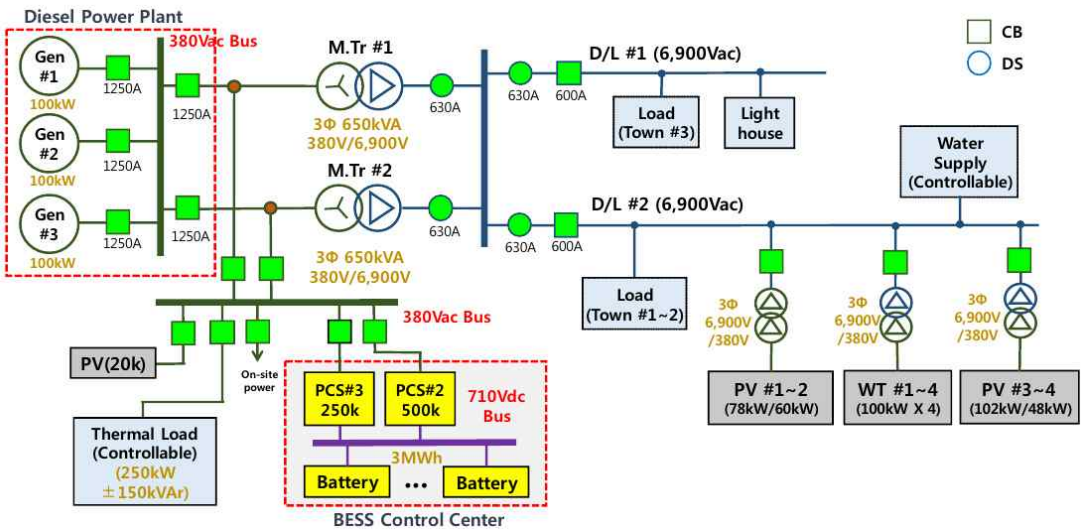

Fig. 8. Single-line diagram of electric circuit model of Gasa Island microgrid

q is the charge of electron (C), V is PV output voltage (V), R_s is series resistance (Ω), R_{sh} is shunt resistance (Ω), k is Boltzmann's constant (J/K), and A is the ideality factor. This model has been widely used by researchers [32-33].

4.4.4 Wind turbine model

We modeled type-IV wind turbine (WT) that utilizes a permanent magnet synchronous generator model (PMSG), AC/DC/AC back-to-back converter model, and maximum power point tracking (MPPT) controller model for maximum wind energy capture [34].

Because the wind speed fluctuates randomly, there are regulations on the output of WT system in the grid code. According to the grid code, the WT system must be able to limit the power output and ramp rate and have low-voltage-ride-through (LVRT) capability. To meet this requirement, we implement a robust PLL scheme referred to as the Decoupled Double Synchronous Reference Frame PLL (DDSRF-PLL) proposed by [35] and fast fault detection method [36].

5. Field Test and Simulation Results

5.1 Simulation results

To verify the voltage and frequency control schemes of microgrid considering coordination of the BESS and diesel generators, we set up simulation model of the Gasa Island microgrid in MATLAB/Simulink. In normal operation, the BESS operates in CVCF mode. Therefore, it will instantly compensate load variation. Diesel generators serve as a backup generator to keep BESS SoC within the desired range. On top of it, during an abnormal condition when BESS cannot respond to load changes due to inadvertent faults or scheduled maintenance, diesel generators operate as the master source with P-f droop control mode.

Three scenarios are simulated in this paper. Simulation scenario 1 examines the effectiveness of the CVCF control of the BESS during load changes. In simulation scenario 2, the load was kept constant while power from PV and wind turbine changes abruptly. The effect of BESS trip is investigated in scenario 3. In scenario 3, we simulate conventional voltage and frequency control by diesel generators so that comparison can be made with the CVCF control of BESS adopted in this paper.

5.1.1 Simulation scenario 1: Effects of load variation

In this simulation scenario, the load varies abruptly while the renewable power from PV and wind turbine are kept constant. As shown in Fig. 9, at 15.0 s, the total load in the microgrid suddenly increases more than 20% from 83 kW to 101 kW. The BESS operated in CVCF mode quickly responds to this change by increasing its output power from 11 kW to 29 kW. At 20.0 s, the load suddenly

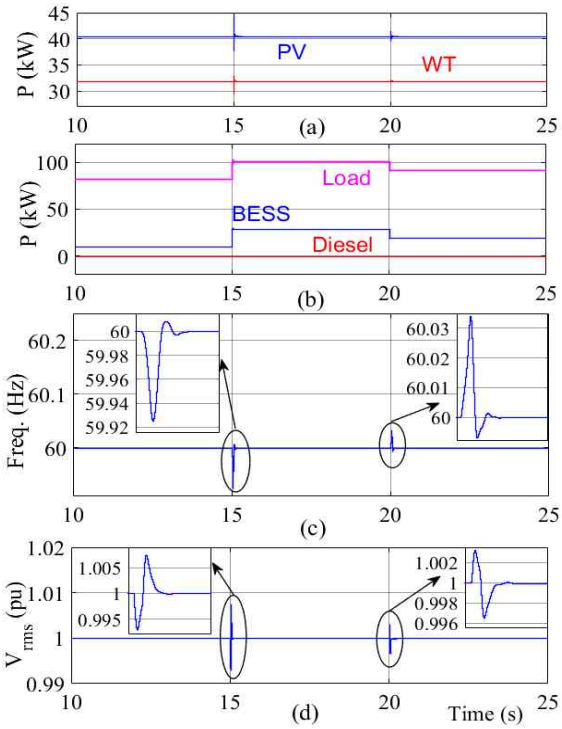

Fig. 9. Results for simulation scenario 1: (a) Active power of PV and WT, (b) Active power of BESS, diesel generator and load, (c) System frequency, (d) RMS output voltage of BESS

drops by 10 kW to 91 kW. Then, the BESS can also instantly respond by reducing its output power from 29 kW to 19 kW in order to balance the power change.

The system frequency and voltage measured at the BESS connection point are shown in Fig. 9. It can be observed that both the system frequency and voltage can remain constant with small transients from the nominal values such as 60 Hz and 1.0 p.u., respectively during load changes.

5.1.2 Simulation scenario 2: Effects of renewable energy fluctuation

To ensure that the proposed scheme works well with renewable energy variation, we simulate variation of both wind speed and solar radiation while keeping the load constant at the average load of 90 kW. Solar radiation is decreased from 200 W/m² to 150 W/m² at 15.0 s and wind speed is increased from 6 m/s to 7 m/s at 20.0 s.

As can be observed from Fig. 10, the active power of PV drops from 40 kW to 30 kW at 15.0 s. The BESS compensates this shortage by increasing its power output and therefore power balance of the microgrid can be maintained. At 20.0 s, wind turbines suffer sudden jumps in their total output power from 32 kW to 43 kW with an increase of 11 kW. This increase leads the BESS to decrease its active power by 11 kW. The system frequency and voltage measured at the BESS can remain constant at

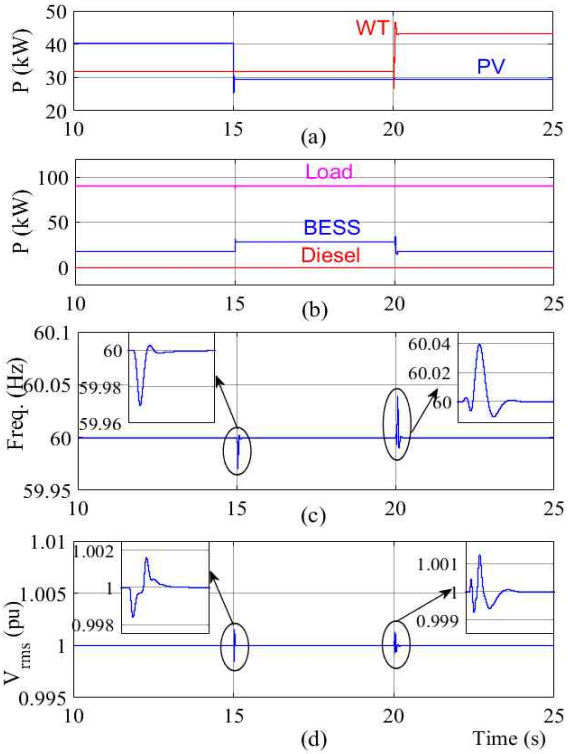

Fig. 10. Results for simulation scenario 2: (a) Active power of PV and WT; (b) Active power of BESS, diesel generator and load; (c) System frequency; (d) RMS output voltage of BESS

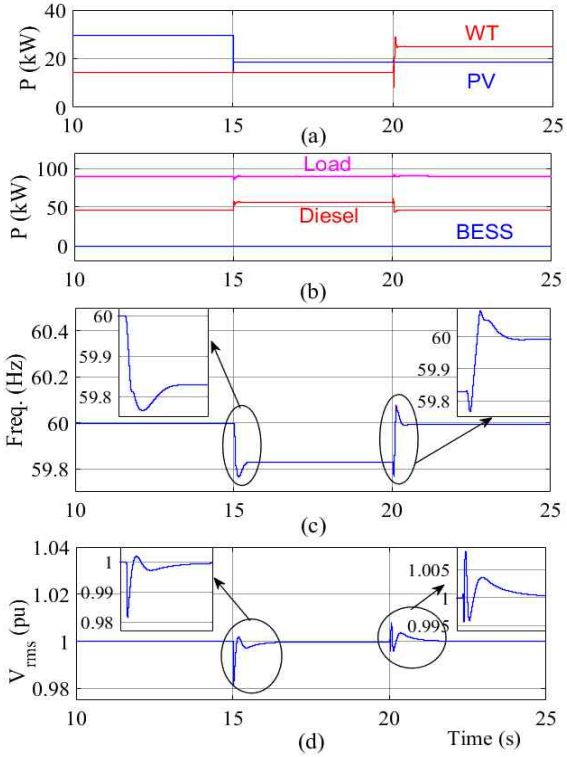

Fig. 11. Results for simulation scenario 3: (a) Active power of PV and WT, (b) Active power of BESS, diesel generator and load, (c) System frequency, (d) RMS output voltage of BESS

60 Hz and 1.0 p.u, respectively, as shown in Fig. 10.

5.1.3 Simulation scenario 3: Tripping of BESS

Since the BESS is the main component that controls the system voltage and frequency, its reliability and security are important. In this case, we simulate a scenario where BESS is unavailable due to unexpected faults or inevitable maintenance. Then, diesel generators must serve as the main power source by controlling the system frequency. In this case, real and reactive power mismatch can be compensated by autonomous parallel operation of diesel generators. However, the system frequency and voltage can suffer slight variation due to the characteristics of droop controls.

The scenario is simulated as follows: in the beginning of the simulation, solar radiation and wind speed are 150 W/m² and 5 m/s, respectively. One diesel generator is on and runs in droop mode by controlling the voltage and frequency. At 15.0 s, power output from PV suddenly drops and wind turbine power output increases at 20.0 s. We assume that the load demand is constant at 90 kW. Since the BESS is unavailable, the diesel generator will be responsible for compensating any power imbalance. In order to clearly demonstrate the performance comparison with the two previous scenarios, the load reference commands for the diesel generator are chosen so that the initial values of the system frequency and voltage are set to 60.0 Hz and 1.0 p.u., respectively.

Fig. 11 shows the simulation results of scenario 3. The system frequency and voltage are measured at the BESS connection point. As shown in Fig. 11, the microgrid can securely supply electric power to the loads under power variation of RESs. Other than the former two scenarios, we can observe more transients and variations in the system frequency and voltage but they can be maintained within acceptable regions, which is less than 0.2 Hz in this scenario.

It is clear that scenarios 1 and 2, where BESS is the main source, can provide better quality performances in terms of frequency deviation and faster response to power imbalance.

5.2 Field measurements from real-world microgrid installed in Gasa Island

KEPCO has completed the construction of the microgrid system in Gasa Island in October 2014 and it has been in successful operation since then. Table 9 lists the specification of components in the microgrid. The design of the microgrid is consistent with our former result almost the same as case 5 in Table 6. The difference from case 5 is an additional 500 kVA BESS inverter for test purposes. PV panels are scattered over the island. Three diesel generators

Table 9. Specification of Gasa Island microgrid

Category	Quantity	Description
EMS	1 system	Renewable energy estimation, Automatic source control, demand control
BESS Inverter	500kVA x 2 250kVA x 1	CVCF control, PQ control
BESS	3 MWh	Life span: 4,000 cycle
WT	100kW x 4	PMSG with full-scale converter (Type-IV) with P limit control, LVRT, and power factor correction
PV	314 kW total (incl. 78/60/102/48/17/3/3/3kW)	P limit control
Diesel generator	100kW x 3	Droop control (installed already before the project)

Fig. 12. Image of the microgrid operating center in Gasa Island

had been already installed and energized the island before this microgrid project.

Fig. 12 shows the site image of the central operating center of Gasa Island microgrid established near the BESS and diesel generators. The screens on the wall in Fig. 12 shows the monitoring data and system conditions of EMS developed by KEPCO. The EMS includes multiple state-of-the-art functions for island microgrids such as renewable energy estimation, automatic source control for BESS, diesel generators and other energy resources, demand control for electric heaters, air conditioners, and fish farms.

In order to prove the effectiveness of our control approach, we recorded and analyzed one-year operation data (from January to December 2015). The data include voltage, current, active power, reactive power, power factor, and system frequency. Fig. 13 shows 5-second windows of the test measurement data to see the effect of fast and short-term intermittency of renewable energy. The data was measured at 19:03pm on September 2, 2014. The sampling time of the graphs is 0.1 seconds. From Fig. 13 (a) and (b), we can see the peak frequency deviation is within 5 mHz, and the peak deviation of 3-phase line-to-neutral voltage is 0.002 p.u. The active and reactive power are shown in Fig.13 (c). In this measurement, three wind turbines are generating power and the load is around 90kW. The surplus power in the microgrid is charged to the BESS as shown in Fig. 13 (c).

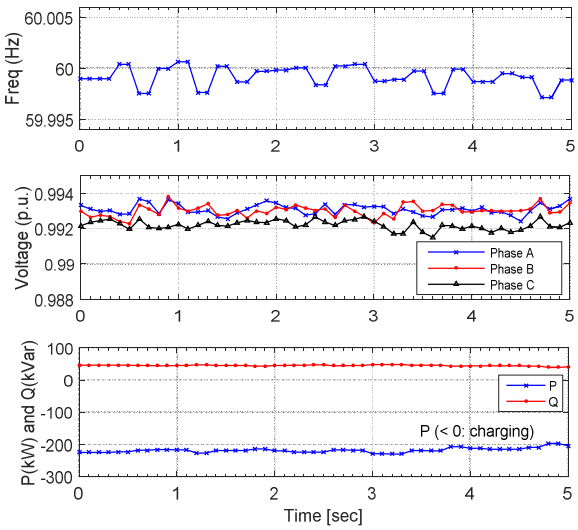

Fig. 13. Measurement data at the BESS connection point in Gasa Island for 5 seconds from 19:00pm (sampling time=0.1 seconds): (a) system frequency in Hz, (b) 3-phase line-to-neutral voltages in p.u., (c) active and reactive power in kW and kVar

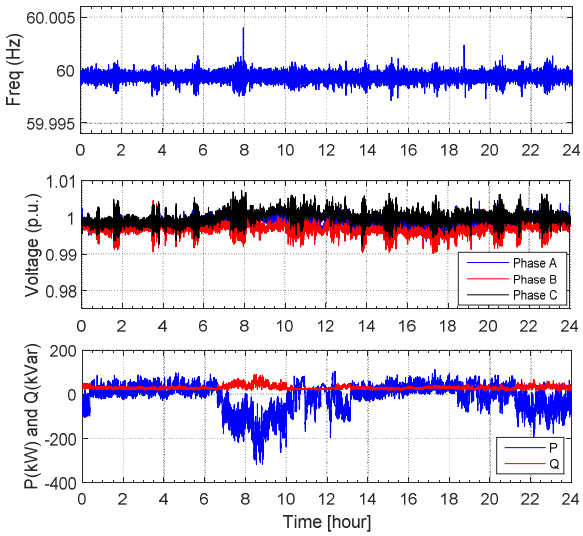

Fig. 14. Measurement data at the BESS connection point in Gasa Island for 24 hours from 00:00 am (sampling time = 3 seconds): (a) system frequency in Hz, (b) 3-phase line-to-neutral voltages in p.u., (c) active and reactive power in kW and kVar

Fig. 14 demonstrates the measurement data for a 24-hour period with a sampling time of 3 seconds. The data was measured from 00:00:00am to 23:59:59pm on January 8, 2015. During this time, the load and renewable energy continuously vary throughout the day. The frequency and voltage peak deviation remain within 10 mHz and 0.02 pu, respectively. Fig. 14 (c) shows active and reactive power balanced despite continuous variation of load and renewable energy throughout the day.

6. Conclusion

This paper presents the design and dynamic performance of KEPCO's stand-alone microgrid in Gasa Island, South Korea. We use BESS to control the system frequency and voltage instead of the conventional approach of using synchronous generators. This makes the microgrid immune to mechanical inertia and the fast response of BESS to power imbalance results in better dynamic performance. This feature can permit high penetration of renewable energy and therefore reducing greenhouse gas emission. Despite these benefits, however, the drawback of this technique is the cost of BESS and power electronic devices. We addressed this issue by performing detailed sizing/economic analysis and come up with an optimal storage capacity. Our analysis shows that achieving 100% renewable energy penetration is not economically viable.

The scheme was demonstrated and verified via dynamic simulation studies. We found out that with the current technology and economics of BESS, our approach cannot be applied to bigger stand-alone microgrids as the BESS cost will become infeasible. However, as we pointed out in the paper, this approach is more suitable for a small stand-alone microgrid like Gasa Island that has low system inertia and environmentally clean area. We discussed real operation results from the microgrid.

According to a two-year operation, KEPCO expects to save diesel fuel consumption as much as 300,000 US dollars every year and tremendous reduction in greenhouse gas emission. In addition, the residents are satisfied with the improved quality of electricity. Learning from the successful Gasa Island initiative, South Korea is replicating the microgrid model and scaling it up on other bigger islands such as Ulleung Island.

Acknowledgements

This work was supported by the National Research Foundation of Korea (NRF) grant funded by the Korea government (MSIP) [NRF-2015R1C1A1A01054635], the Korea Institute of Energy Technology Evaluation and Planning (KETEP) grant funded by the Ministry of Trade, Industry & Energy of Korea [No.20151210200080], and the Global Scholarship Program for Foreign Graduate Students at Kookmin University.

References

[1] S. K. Singal, R.P. Singh, "Rural electrification of a remote island by renewable energy sources," *Renewable Energy*, vol. 32, pp. 2491-2501, 2007.

[2] D. Neves, C.A. Silva, S. Connors, "Design and implementation of a hybrid renewable energy systems on micro-communities: A review of case studies," *Renewable and Sustainable Energy Review,* vol. 31, pp. 935-946, 2014.

[3] W. Zhou, C. Lou, Z. Li, L. Lu, and H. Yang, "Current status of research on optimum sizing of stand-alone hybrid solar-wind power generation systems," *Applied Energy,* vol. 87, pp. 380-389, 2010.

[4] D. Connolly, H. Lund, B. V. Mathiesen, and M. Leahy, "A review of computer tools for analyzing the integration of renewable energy into various energy systems," *Applied Energy*, vol. 87, pp. 1059-1082, 2010.

[5] S. Sinha, S.S. Chandel, "Review of software tools for hybrid renewable energy systems," *Renewable and Sustainable Energy Review,* vol.32, pp. 192-205, 2014.

[6] B. Zhao et al, "Optimal sizing, operating strategy and operational experience of a stand-alone microgrid on Dongfushan Island," *Applied Energy*, vol. 113, pp. 1656-1666, 2014.

[7] A. Malheiro, P.M. Castro, R.M. Lima, A. Estanqueiro, "Integrated sizing and scheduling of wind/PV/diesel/ battery isolated systems," *Renewable Energy*, vol. 83, pp. 646-657, 2015.

[8] G. Giatrakos, T. Tsoutsos, P. Mouchtaropoulos, G. Naxakis, and G. Stavrakakis, "Sustainable energy planning based on a stand-alone hybrid renewable energy/hydrogen power system: Application in Karpathos Island, Greece," *Renewable Energy*, vol. 34, pp. 2562-2570, 2009.

[9] O. Hafez and K. Bhattacharya, "Optimal planning and design of a renewable energy based supply system for microgrids," *Renewable Energy*, vol. 45, pp. 7-15, 2012.

[10] T. Senjyu, D. Hayashi, A. Yona, N. Urasaki, and T. Funabashi, "Optimal configuration of power generating systems in isolated island with renewable energy," *Renew Energy*, vol.32, pp.1917-1933, 2007.

[11] R. Atia, and N. Yamada, "Sizing and Analysis of Renewable Energy and Battery Systems in Residential Micro-grids," *IEEE Trans. Smart Grid,* vol. 7, pp. 1204-1213, 2016.

[12] M. Stadler, M. Groissbock, G. Cardoso, and C. Marnay, "Optimizing Distributed Energy Resources and building retrofits with the strategic DER_ CAModel," *Applied Energy,* vol. 132, pp. 557-567, 2014.

[13] A. Omu, R. Choudhary, and A. Boies, "Distributed energy resource system optimization using mixed integer linear programming," *Energy Policy,* vol. 61, pp. 249-266, 2013.

[14] M. Barnes, et al, "Real-world microgrids - an overview," *IEEE International Conference on System Engineering*, 2007.

[15] L.C. Chang and Y.C. Yin, "Strategies for operating wind power in a similar manner of conventional power plant," *IEEE Trans. Energy Conversion,* vol.

24, pp. 926-934, 2009.
[16] K. Vidyanandan, and N. Senroy, "Primary frequency regulation by deloaded wind turbines using variable droop," *IEEE Trans. Power System*, vol. 28, pp. 837-846, 2013.
[17] H. Xin, et al, "A new frequency regulation strategy for photovoltaic systems without energy storage," *IEEE Trans. Sustain. Energy*, vol. 4, pp. 985-993, 2013.
[18] Z. Miao, L. Xu, V.R. Disfani, and L. Fan, "An SOC-Based Battery Management System for Microgrids," *IEEE Trans. Smart Grid*, vol. 5, pp. 966-973, 2014.
[19] I. Serban and C. Marinescu, "Control Strategy of Three-Phase Battery Energy Storage System for Frequency Support in Microgrids and with Uninterrupted Supply of Local Loads," *IEEE Trans. Power Electronics*, vol.29, pp.5010-5020, 2014.
[20] Y. Xu, W. Zhang, G. Hug, S. Kar, and Z. Li, "Cooperative Control of Distributed Energy Storage Systems in Microgrid," *IEEE Trans. Smart Grid*, vol. 6, pp. 238-248, 2015.
[21] Y. Han, P. M. Young, and A. Jain, "Robust Control for Microgrid Frequency Deviation Reduction with Attached Storage System," *IEEE Trans. Smart Grid*, vol. 6, pp. 557-565.
[22] T. Morstyn, B. Hredzak, and V.G. Agelidis, "Distributed Cooperative Control of Microgrid Storage," *IEEE Trans. Power Systems*, vol. 30, pp. 2780-2789, 2015.
[23] P. Lilliental, T. Lambart, and G. Paul, *Integration of Alternative Sources of Energy*, IEEE-Wiley Press.
[24] KEPRI, *Final Report for Development of Convergence and Integration Technology for Renewable-Based Energy System and Its Grid Interconnection*, KEPCO, Daejeon, Korea, 2015
[25] W. Chae, H. Lee, J. Won, J. Park, and J. Kim, "Design and Field Tests of an Inverted Based Remote Micro-Grid on a Korean Island," *Energies*, vol. 8, pp. 8193-8210, 2015.
[26] P. Kundur, *Power System Stability and Control*, McGraw-Hill 1994.
[27] C. Zhu, X. Li, L. Song, and L. Xiang, "Development of a theoretically based thermal model for lithium-ion battery pack," *Journal of Power Sources*, vol. 223, pp. 155-164, 2012.
[28] J. Rocabert, A. Luna, F. Blaabjerg, and P. Rodriguez, "Control of power converters in AC microgrids," *IEEE Trans. on Power Electronics*, vol. 27, pp. 4734-4749, 2012.
[29] P. Krause, *Analysis of Electric Machinery*, McGraw-Hill 1986.
[30] *IEEE Standard Definitions for Excitation Systems for Synchronous Machines*, 2007
[31] H. Rauschenbach, *Solar Cell Array Design Handbook*, New York: Van Nostrand Reinhold 1980.
[32] G. E. Ahmad, M. Hussein, and H. Ghetany, "Theoretical analysis and experimental verification of PV modules," *Renewable Energy*, vol. 28, pp. 1159-1168, 2003.
[33] D. Sera, R. Teodorescu, and P. Rodriguez, "PV panel model based on data sheet values," in Proc. *IEEE Int. Symp. Ind. Electron.*, pp. 2392-2396, 2007.
[34] C. Yoo, I. Chung, H. Lee, and S. Hong, "Intelligent control of battery energy storage for multiagent based microgrid energy management," *Energies*, vol. 6, pp. 4956-4979, 2013
[35] P. Rodriguez, J. Pou, J. Bergas, J. Candela, R. Burgos, and D. Boroyevich, "Decoupled Double Synchronous Reference Frame PLL for Power Converters Control," *IEEE Transactions on Power Electronics*, vol. 22, pp. 584-592, 2007.
[36] C. Yoo, I. Chung, H. Yoo, and S. Hong, "A Grid Voltage Measurement Method for Wind Power Systems during Grid Fault Conditions," *Energies*, vol. 7, pp. 7732-7745, 2014.

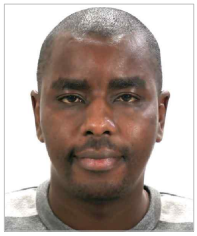

Munir Husein received B.Eng. and M.S degrees in electrical engineering from Bayero University at Kano, Nigeria and Yasar University at Izmir, Turkey. He is currently working towards his Ph.D degree at Smartgrid and Power Systems Lab, Kookmin University, Seoul. His research interests include distributed generation and microgrid design and analysis.

Vu Ba Hau received Bachelor's degree in automatic control engineering from Hanoi University of Science and Technology, Hanoi, Vietnam, in 2015. Currently, he is a master student in the School of Electronics Engineering, Kookmin University. His research interests are microgrid design and analysis.

Il-Yop Chung received B.S., M.S., and Ph.D. degrees in electrical engineering from Seoul National University, Seoul, Korea, in 1999, 2001, and 2005, respectively. He was a Postdoctoral Associate at Virginia Tech, Blacksburg, VA, USA from 2005 to 2007. From 2007 to 2010, he worked for the Center for Advanced Power Systems at Florida State University, Tallahassee, FL, USA as an Assistant Scholar Scientist. Currently, he is an Associate Professor at Kookmin University, Seoul, Korea.

Woo-Kyu Chae received the B.Eng. degree from Sungkyunkwan University and the M.S. degree from Chungbuk National University, Korea, in 2007. He also finished the doctorial course in Chungbuk National University in 2014. He is a senior researcher and electrical engineer in KEPRI (Korea Electric Power Research Institute) from 2004, Korea. His research activity is focused on the design and control of Microgrid and renewable energies

Hak-Ju Lee received B.S.,M.S.,and Ph.D. degrees in electrical engineering from Chungnam National University in Korea, in 1989,1991 and 2004, respectively. Currently He is a principal research member of Energy & New Industry Lab. in KEPCO. His research interests are design & analysis of microgrid, power converter for distribution power systems.